Improved Automatic Registration Adjustment of Multi-source Remote Sensing Datasets

Rawaa Abdul Jabbar Mohammed
Engineer
College of Engineering - Diyala University
rrr_rys_1979@yahoo.com

Dr. Fanar Mansour Abed
Lecturer
College of Engineering- Baghdad University
fanar.mansou@coeng.uobaghdad.edu.iq

Dr. Loay Edwar George
Assistant professor
College of Science - Baghdad University
loayedwar57@yahoo.com

ABSTRACT

Registration techniques are still considered challenging tasks to remote sensing users, especially after enormous increase in the volume of remotely sensed data being acquired by an ever-growing number of earth observation sensors. This surge in use mandates the development of accurate and robust registration procedures that can handle these data with varying geometric and radiometric properties. This paper aims to develop the traditional registration scenarios to reduce discrepancies between registered datasets in two dimensions (2D) space for remote sensing images. This is achieved by designing a computer program written in Visual Basic language following two main stages: The first stage is a traditional registration process by defining a set of control point pairs using manual selection, then comput the parameters of global affine transformation model to match them and resample the images. The second stage included matching process refinement by determining the shift value in control points (CPs) location depending on radiometric similarity measure. Then shift map technique was adjusted to adjust the process using 2nd order polynomial transformation function. This function has chosen after conducting statistical analyses, comparing between the common transformation functions (similarity, affine, projection and 2nd order polynomial). The results showed that the developed approach reduced the root mean square error (RMSE) of registration process and decreasing the discrepancies between registered datasets with 60%, 57% and 48% respectively for each one of the three tested datasets.

KEY WORDS: Remote Sensing, Registration, Matching, Similarity Measure, Adjustment

تحسين عمليات تسجيل بيانات التحسس النائي آلياً

د. فنار منصور عبد
مدرس
كلية الهندسة- جامعة بغداد

د. لؤي ادورد جورج
استاذ مساعد
كلية العلوم- جامعة بغداد

رواء عبد الجبار محمد
مهندس
قسم الشؤون الهندسة- جامعة ديالى

الخلاصة

تقنية التسجيل لازالت تعتبر من المهام الصعبة لمستخدمي بيانات التحسس النائي خصوصا بعد الزيادة الهائلة بحجم البيانات المكتسبة من الاعداد المتزايدة والمطورة للمتحسسات وهذه الطفرة بحاجة لتطويروتحسين دقة وقوة خطوات التسجيل التي بامكانها التعامل مع هذه البيانات المختلفة الخصائص الراديومترية والهندسية . يهدف هذا البحث الى تطوير وتحسين عملية التسجيل التقليدية لتقليل الفرق بين البيانات المسجلة في المجال الثنائي الابعاد لصور التحسس النائي. هذا يتحقق من خلال تصميم برنامج بلغة visual basic باتباع مرحلتين اساسيتين: الاولى هي القيام بعملية التسجيل بالطريقة التقليدية من خلال تحديد مجموعة من أزواج نقطة الضبط باستخدام الاختيار اليدوي، ثم حساب ثوابت موديل التحويل العالمي affine لمطابقة واعادة تشكيل الصور. المرحلة الثانية تتضمن عملية تحسين المطابقة بقياس مقدارالازاحة لمواقع نقاط الضبط بالاعتماد على قياس التشابه الراديومتري ومن ثم تم تحسين تقنية shift map لتحسين عملية التسجيل باستخدام دالة التحويل 2nd order polynomial والتي تم اختيارها بعد اجراء تحليل احصائي والمقارنة بين اكثر الدوال شيوعا . أظهرت النتائج أن النهج المطور خفض RMSE من عملية التسجيل وقلل الاختلاف بين مجموعة البيانات المسجلة بنسبة 60٪، 57٪ و 48٪ على التوالي لكل واحدة من مجموعة البيانات الثلاثة التي تم اختبارها.

الكلمات الرئيسية: التحسس النائي، تسجيل الصور، موائمة الصور، معامل التشابه، تصحيح الصور

INTRODUCTION

Image registration is a process to determine the geometric transform that aligns points of a certain object in one view with the corresponding points of that object in another view to minimize position shifting errors. This process is often necessary for integrating information taken from different sensors, transponders, finding changes in images taken at different times, elevation or under different conditions. This is applied for model based object recognition and inferring three-dimensional information from images in which either the camera on satellite or the objects in the scene has moved **Singhai, R. and Singhai, J., 2012**. Images registration remains challenging for several reasons. First, images are usually acquired using different sensor types, each having its inherent noise. Furthermore, radiometric as well as geometric properties of the same objects in the involved imageries might differ as a result of changes in the sensor view point, imaging methodology, imaging conditions (e.g., atmospheric changes, cloud coverage, and shadows), and spectral sensitivity of the implemented imaging systems (e.g., panchromatic, multi- and hyper-spectral imaging systems) **Jensen, 1986; Jia, 2003**. Finally, the registration process can be complicated because of changes in object space caused by movements, deformations, and urban development between the epochs of capture associated with the involved images **Martinez and Abad, 2000**.

In general, any image registration methodology must deal with four issues. First, the choice of primitives for the registration procedure. Then, establishing the registration transformation function that mathematically related the images under consideration. The third issue concerns the similarity measure which should be devised to ensure the correspondence of the conjugate primitives. Finally, after establishing the registration primitives, transformation function, and similarity measure, one should focus on how to establish the correspondence between conjugate primitives. Corresponding primitives in the reference and input images can be identified manually. The need for fast registration methods mandates the automation of the process of identifying conjugate primitives **Alruzouq, R.I., 2004**. Therefore, a matching strategy has to be developed to manipulate the registration primitives, the transformation function, and the similarity measure to automatically establish the correspondence between conjugate primitives.

In this paper, a developed matching strategy is adopted to attain high accuracy for image registration process. There are several attempts to improve image registration. **Wong, A., 2007**; presented an automatic registration method for remote-sensing images obtained at different times and/or from different sensors. The introduced method uses a set of features that are invariant to intensity mappings during the control-point matching process. He addressed global and local contrast issues associated with remotely sensed images and intensity-difference issues associated with multimodal registration of remotely sensed images. **Wong, A., 2008**; referred that the error residue can be minimized by applying a combination of efficient globally exhaustive optimization techniques and subpixel-level locally optimization techniques. This combination can further improve robustness in situations with small initial overlap. **Sang, L., 2010**; introduced automatic coarse-to-fine image registration algorithm for satellite images, based on Haar Wavelet Transform (HWT) and the Speeded Up Robust Features (SURF) algorithm in the coarse registration. He used the normalized cross-correlation and Random Sample Consensus (RANSAC) algorithm to achieve fine registration. However, **Gang, H. and Yun, 2008**; introduced image registration technique, which is based on wavelet-based feature extraction technique, a normalized cross-correlation matching and relaxation-based image matching techniques. On the other hand, **Fatiha, M. et al., 2010**; presented an efficient image registration algorithm that is based on using genetic algorithms and the cross-correlation similarity measure

for matching within a multi-resolution framework based on the Non-Subsampled Contourlet Transform (NSCT).
In this paper, a developed image registration of remote sensing images was presented, based on two main steps; first steps is traditional registration using manually selection of control points and global affine transformation model to match them and second stage; matching process refinement by determining a shift map using 2nd order polynomial transformation function. Whereas the shift values were calculated for CPs by applying radiometric similarity measure. The remainder of this paper was organized as follows; data sets and study sits used was described in section two. The methodology was discussed in detail in section three; the obtained results were presented in details in section four and conclusions discussed in section five.

1. STUDY SITES AND DATA SETS

Three sets of remote sensing data have been derived from Digital Globe and used in this research. The utilized datasets can be divided into two categories; data from different passive panchromatic sensors and data from active LiDAR systems. Then data from passive sensors include Spot satellite image and Quick Bird panchromatic image, as shown in **Fig. 1.a** and **Fig. 1.b** respectively. Both acquired over Ramadi city and they are having 2.5 m and 0.6 m spatial resolution respectively. In this test set, a rural area was used to test adjusted process capability of making more accurate registration process. The size of images (a) is 2501 x 2698 pixels, and the size of image (b) is 1259 x 1545 pixels. The second set data was Panchromatic image from Ikonos satellite as shown in **Fig.2.a** and the corresponding panchromatic image from Quick Bird satellite as shown in **Fig. 2.b**. Both acquired over Baghdad city; they have 1.0 m and 0.6 m spatial resolution respectively. In this test set, an urban area was used to test the method capability of registering data of dense area, the size of image (a) is 1492 x 1508 pixels and the size of image (b) is 1288 x 1501 pixels. Third test data was LiDAR data sets over Niagara city in USA acquired with 1km flying height and delivered as LAS data format from the Finnish terrasolid company (www.Terrasolid.com) for training purposes. Laser point clouds data sets of two overlapping flight lines are shown in **Fig. 3.a** and **3.b** respectively.

2. METHODOLOGY

A developed registration technique for different remote sensing data source are critically needed, because an enormous increase in the volume of remote sensing data being acquired by an ever-growing number of earth observation sensors. In this section, the developed methodology of the adjusted registration process is presented including the traditional registration process, the statistical analyses, and the refinement of images matching process by shift map using 2nd order polynomial for satellite images and LIDAR data are presented as shown in **Fig 4**.

3.1 Transform the 3D LiDAR Data into 2D Images

LiDAR data is 3D digital representation of the scanned features. It has transformed into two dimension images using QTM software for next registration process steps. This is achieved by generating digital surface model, interpolate the surface and export the surface as 2-D images as shown in **Fig 5**.
The LAS files containing the LiDAR data points which require further manipulation to generate a DSM.

3.1.1 Grid Size for Digital Surface Models

Before generating any LiDAR derived Digital Surface Model (DSM), selection of grid size for DSM raster layer is crucial for minimizing the data loss during conversion **Kumar V., 2012.**

The optimized DSM resolution must match the density of LiDAR data and should able to reflect the variability of the terrain surface to represent the majority of terrain features. **Liu, 2008 and McCullagh**, **1988** suggested that the number of grids should be roughly equivalent to the number of LiDAR points in the covered area. The grid resolution (S) of a DSM can be estimated using **Eq. (1) Hu et al., 2003**:

$$S = \sqrt{\frac{A}{n}} \quad (1)$$

where n is the number of terrain points and A is the covered area. This means that the DSM resolution should match the sampling density of the original terrain points.

3.1.2 Model Selection

The points used to generate surfaces by different model selections have been developed to represent surfaces: regular grid (usually square grid); triangular irregular network (TIN); and contour line model. However, it introduces discontinuity in representation of the terrain surfaces due to same elevation value. This effect is minimized by the high density characteristic of LiDAR data **Liu, 2008**

The simplest way to generate a closed surface from the point cloud is by triangulation process, and it is a method used in QT Modeler software v.5.1.5, where every three adjacent 3D points combine to form a triangular surface element. Delaunay triangulation offers an appropriate method of creating such a triangular mesh. This identifies groups of three neighboring points whose maximum inscribed which circle does not include any other surface point. Each triangle can be defined as a plane in space using **Eq. (2)** and the result is a polyhedron representation or wire model of the surface. There is normally has no topological relation between the 3D points. Differential area elements must be established between adjacent points in order to generate a topologically closed surface which enables further processing as a surface description. All 3D points on the plane are defined by the following equation:

$$a(x - x_0) + b(y - y_0) + c(z - z_0) = 0 \quad (2)$$

where:
x,y, z are the coordinates of each point.
x_0,y_0, z_0 are the coordinate of the origin point.

3.1.3 DSM Interpolation

Interpolation is the process of predicting the values of certain variable using their neighboring values. It is assumed that a terrain surface is continuous and that a high correlation exists between the neighboring data points. Interpolation methods are classified into deterministic such as Inverse Distance Weighted (IDW) and spline-based and geostatistic such as Kriging. **Liu, 2008** found there is no single interpolation method that is the most accurate one in all cases.

After DSM is created, the surface is exported as two dimensions (image) as 24-bit intensity color – TIF format. This process delivers two images for Niagara city ready for insertion to the developed registration program.

3.2 Comparison between Common Transformation Methods

In order to assess the accuracy of the selected transformation methods, polynomial, affine, conformal and projection methods, a set of selected distinct feature points extracted from datasets have been tested and validated statistically. The analysis aimed to investigate the deviation of the mean values between CPs in the overlapping region delivered from each method

individually. This allows for inspection of discrepancies between individual feature points in the overlapping regions in both reference and sensed images after transformation. In order to compare between the four transformation methods, (30) feature points from sensed and reference images were selected and the parameters of the transformation function for each method were calculated using least square criterion as shown in **Table 1**. The coordinates of the control points belong to the sensed image are mapped to the coordinate system of the reference image. After the determination of transformation function coefficients, optimization method was applied that is based on statistical bases to adjust the geometric errors. T-test statistical method is used to compare the matched pairs of the coordinates.

Before this analysis, we must check the comparative dataset variances using F-test. Testing means and variances of the discrepancies between the selected feature points from both matched pairs are translated by P-values indicators to show the accuracy and the degree of confidence of matching process. All these statistical analysis should be applied after testing the degree of confidence of how well these data are normally distributed and fitted with the normal distribution curve. This is an essential step to make sure that the statistical hypothesis and the delivered results are valid for the current datasets. These tests determine the appropriateness of accepting or rejecting the null hypothesis which assumes the data are similar and perfectly matched based on P-value reports. If the p-value of a statistical test is less than 0.05, we reject the null hypothesis. From the T-test results shown in **Table 2**. it can be realized that the 2^{nd} order polynomial transformation method is the best transformation function to use with our current datasets. Following these results, this function was used in the developed images registration process to correct the geometric shift.

3.3 Images Registration Process

In this stage, the traditional registration process is conducted and it is consists of four steps; manual selection of CPs, transformation function, similarity measurement, and matching with resample image registration.

3.3.1 Manual Feature Extraction and Selection

Choosing points of interest within the image pixel space is not an easy task, because we need to easily identify significant and distinct high-level features such as line intersections, road crossings, centroids of water regions, oil and gas pads, high variance points, local curvature discontinuities, curve inflection points, most distinctive points of similarity measure, etc. ., which are possibly uniformly spread over the images and easily detectable, as shown in **Fig 6, 7, and 8.**

3.3.2 Two-dimensional Transformation Method

Two-dimensional (2D) transformation is transforming the coordinates of points in one rectangular system (x, y) into coordinates in another rectangular system (X, Y) **Deakin, 2004**.
After the feature correspondence has been established, the mapping function is constructed. It should transform the sensed image to overlay it over the reference one. The CP from the sensed image that the corresponding CP from reference images should be as close as possible after the sensed image transformation is employed in the mapping function design. The task in this stage consists of choosing the type of the mapping function and its parameter estimation. The most fundamental characteristic of any image registration technique is the type of spatial transformation or mapping needed to properly overlay two images. Although many types of distortion may be present in each image, the registration technique must select the class of transformation which will remove only the spatial distortions between images due to differences in acquisition and not due to differences in scene characteristics to be detected. The primary

general transformations are affine, projective, conformal, and high order polynomial. These are all well-defined mappings of one image into another **Brown, 1992 and Zitova and Flusser, 2003**. In this research affine transformation has used in the first stage (traditional registration) as shown its parameters in **Table 3,4 and 5** sequentially for each one of the three tested datasets and 2nd order polynomial transformation has used in the second stage (adjusted registration) as shown its parameters in **Table 6** for the three tested datasets.

A. Affine Transformation

Affine transformation is also used for the mapping of two coordinate systems in 2D plane. This 6-parameter transformation defines two displacements, one rotation, and two separate scaling factors as shown in **Fig. 9**.

For a point P in the source system, the XY coordinates in the target system are given by **Eq. 3 and 4. Ghosh, 1979 and Luhmann et al., 2011**:

$$X = a_0 + a_1 x + a_2 y \quad (3)$$
$$Y = b_0 + b_1 x + b_2 y \quad (4)$$

or in non-linear form with $a_0 = X_0$ and $b_0 = Y_0$ as

$$X = X_0 + m_X x \cos\alpha - m_y y \sin(\alpha + \beta) \quad (5)$$
$$Y = b_0 + m_X x \sin\alpha + m_y y \cos(\alpha + \beta) \quad (6)$$

The parameters a_0 and b_0 (X_0 and Y_0) define the displacement of the origin, α and β are the rotation angle, and m_X, m_y are the scaling factors for x and y.

In order to determine the six coefficients a minimum of three identical points is required in both systems. With more than three identical points, the transformation parameters can be calculated by over-determined least-squares adjustment.

In matrix notation, the affine transformation can be written as:

$$X = Ax + a \quad (7)$$

$$\begin{bmatrix} X \\ Y \end{bmatrix} = \begin{bmatrix} a_1 & -b_1 \\ b_1 & a_1 \end{bmatrix} \begin{bmatrix} x \\ y \end{bmatrix} + \begin{bmatrix} a_0 \\ b_0 \end{bmatrix} \quad (8)$$

or

$$\begin{bmatrix} X \\ Y \end{bmatrix} = \begin{bmatrix} m_X x \cos\alpha & -m_y y \sin(\alpha + \beta) \\ m_X x \sin\alpha & m_y y \cos(\alpha + \beta) \end{bmatrix} \begin{bmatrix} x \\ y \end{bmatrix} + \begin{bmatrix} X_0 \\ Y_0 \end{bmatrix} \quad (9)$$

A is the affine transformation matrix. For lightly rotated and sheared systems the parameter a_1 corresponds to the scaling factor m_X and the parameter b_1 to the scaling factor m_y.

B. Polynomial Transformation

Non-linear deformations can be described by polynomials of degree (n), **Fig. 10** shown the Plane polynomial transformations process. In general, the transformation model can be written as **Ghosh, 1979; Luhmann et al., 2011**:

$$X = \sum_{j=0}^{n} \sum_{i=0}^{j} a_{ji}\, x^{j-i} y^{i} \quad (10)$$

$$Y = \sum_{j=0}^{n} \sum_{i=0}^{j} b_{ji}\, x^{j-i} y^{i} \quad (11)$$

where n is degree of polynomial. A polynomial of n=2 are given by:

$$X = a_{00} + a_{10}x + a_{11}y + a_{20}x^2 + a_{21}xy + a_{22}y^2 \quad (12)$$
$$Y = b_{00} + b_{10}x + b_{11}y + b_{20}x^2 + b_{21}xy + b_{22}y^2 \quad (13)$$

The polynomial of n=1 is identical to the affine transformation **Eq. (3) and (4)**. In general, the number of coefficients required to define a polynomial transformation of degree n is:
u = (n+1) (n+2) and in order to determine the u coefficients, a minimum of u/2 identical points is required in both systems.

3.3.3 Least Squares Adjustment

The least squares Gauss-Markov adjustment model is based on the idea that the unknown parameters are estimated with maximum probability. Assuming a data set with an infinite number of measured values and normally distributed errors, the following condition for the residuals results should be used **Luhmann et al., 2011**. The sum of the squares of the residuals must be minimized. **Eq. (14)** expresses the fundamental principle of least squares **Charles and Paulr, 2006**:

$$\sum v^2 = v_1^2 + v_2^2 + \cdots + v_n^2 = minimum \quad (14)$$

The following subsections present the matrix methods used in performing a least squares adjustment for the matrix expressions, an analogy will be made with the systematic procedures let a system of observation equations be represented by the matrix notation **Charles and Paulr, 2006**:

$$AX = L + V \quad (15)$$

Where

$$A = \begin{bmatrix} a_{11} & a_{12} & \cdots & a_{1n} \\ a_{21} & a_{22} & \cdots & a_{2a} \\ \vdots & \vdots & \vdots & \vdots \\ a_{m1} & a_{m2} & \cdots & a_{mn} \end{bmatrix}$$

$$X = \begin{bmatrix} x_1 \\ x_2 \\ \vdots \\ x_n \end{bmatrix} \qquad L = \begin{bmatrix} l_1 \\ l_2 \\ \vdots \\ l_m \end{bmatrix} \qquad V = \begin{bmatrix} v_1 \\ v_2 \\ \vdots \\ v_m \end{bmatrix}$$

$x_1, x_2, \ldots\ldots\ldots x_n$ are the unknowns
$a_{11}, a_{12}, \ldots\ldots a_{1n}$ are the coefficients of the unknowns

$$A^{T}AX = A^{T}L \quad \ldots\ldots\ldots\ldots\ldots\ldots\ldots\ldots \text{(16a)}$$

Eq. (16a) can also be expressed as

$$NX = A^{\mathrm{T}}L \quad \text{.....(16b)}$$

Eq. (16a) and **(16b)** produce the normal equations of a least squares adjustment. By inspection, it can also be seen that the N matrix is always symmetric $(i.e\ldots, n_{ij} = n_{ji})$. By employing matrix algebra, the solution of normal equations such as **Eq. (16a)** is:

$$X = (A^{\mathrm{T}}A)^{-1}A^{\mathrm{T}}L = N^{-1}A^{\mathrm{T}}L \quad (17)$$

3.3.4 Measuring Similarity for Image Registration

Similarity measures are used to register images by finding an accurate match between an input image and transformed versions of the reference image. The two types of the similarity measuring techniques are geometric and radiometric similarity measuring discussed in **Brown, 1992**. The similarity measuring used in this research is geometric to measure the degree of matching images in the first stage (traditional registration) and radiometric similarity measuring to determine the discrepancies in Corresponding CPs in the second stage (refine the registration process).

A geometric similarity measure is mathematically describes the fact that conjugate primitives should coincide with each other after application of the proper registration transformation function. Geometric similarity measure depends on the selected registration primitive (e.g., points, linear features, areal regions) as well as the registration transformation function (e.g., 2-D similarity or affine transformation) is expressed as follows **Habib et al., 2001**:

$$x_r - f_{g_x}(x_i, y_i) = 0 \quad (18)$$

$$y_r - f_{g_y}(x_i, y_i) = 0 \quad (19)$$

where f_{g_x} & f_{g_y} represent the registration transformation function. For affine function, the geometric similarity measure is described as follows **Habib et al., 2001**:

$$x_r - a_0 - a_1 x_i - a_2 y_i = 0 \quad (20)$$

$$y_r - b_0 - b_1 x_i - b_2 y_i = 0 \quad (21)$$

Excluding mismatches is one of the tasks connected to image matching. One possibility of how to avoid some of outliers in matching is by setting thresholds for similarity measures. After measuring the amount of similarity measure between the points in the reference and sensed image, the points that have large values have been rejected (at least of similarity) by threshold. An outlier is an observation point that is distant from other observations, as shown in **Fig 11**.

At least, similarities values are not always outliers because they may not be unusually far from other observations. Therefore, the threshold determines the acceptance or rejection of the points and the values larger than these are points of unaccepted similarity and which must be rejected which considered as outliers later on. Using the threshold similarity measures is so needed to excluding the false matches.

3.3.5 Matching Strategy

In photogrammetric and remote sensing, matching can be defined as the establishment of the correspondence between various data sets. The matching problem is also referred to as the

correspondence problem. The datasets involved in matching might include images, maps and GIS data. Image matching process is an important and prerequisite step for many applications, such as image registration, image orientation, DEM generation, orthorectification, data fusion and relative orientation. Matching strategy refers to the concept or overall scheme of the solution of the matching problem **Schenk, 1999**. It encompasses the selected primitives, transformation functions and similarity measures for solving the registration problems automatically.

3.3.6 Images Re-sampling Techniques

Image re-sampling is a process by which new pixel values are interpolated from existing pixel values whenever the raster's structure is modified such as during projection, datum transformation, or cell resizing operations **Wade and Sommer, 2006**.

Bilinear filtering is a method used to smooth out when the images are displayed larger or smaller than they actually are. Bilinear filtering uses points to perform bilinear interpolation. This is done by interpolating between the pixels nearest to the point that best represents that pixel. Bilinear re-sampling interpolation takes a weighted average of pixels in the original image nearest to the new pixel location. The averaging process alters the original pixel values and creates entirely new digital values in the output image **Santhosh et al., 2010**.

3.4 The Registration Adjustment Following Images Matching Process

After establishing the registration primitives, transformation function, similarity measure, and matching scenario, the second stage is due in order to adjusted matching strategy that has been developed to manipulate the registration primitives, the transformation function, and the similarity measure.

In this stage, the matching strategy has been developed by determining the shift value of CPs through dependence on concept of radiometric similarity measure and using shift map for adjusting matching process using 2^{nd} order polynomial transformation.

Radiometric similarity measure describes the degree of similarity between the gray level distribution functions at the vicinity of the selected point. Small windows composed of gray values serve as primitive points where the center pixel of the window can be used for the definition of the location of a point **Habib et al., 2001**.

An image patch cut from one image, so called template, is searched in the second image. The template consists of m x n pixels, mostly m=n. The position of the template is referred to as the central pixel that is why m and n are odd numbers. The template is compared with patches of the same size in the second image. An approximate position of the corresponding point in the second image can be derived (e.g. when approximations of orientation parameters of two overlapping images are known). The comparison is then restricted to an area called a search area or window. Geometric distortions caused by relief and different orientation of images will influence the matching of large templates, and in order to get acceptable results, a size of the template has to be small, therefore a template of 3x3 pixel size has been selected. However, the size of the search window depends on how precise it is located. Whereas a search window of 7x7 pixel size was used. A value of a similarity measure is calculated at each position of the template within the search window.

Depending on the similarity measure, a corresponding point to the center of the template is assumed to be in the position where maximal value of the similarity measure is obtained.

The sum of absolute differences (SAD) is used which is a known criteria for similarity measure. These criteria represent a quantitative measure of how well conjugate points correspond to each other.

In digital image processing, the sum of absolute differences, defined in **Eq. (22)** as shown in **Ulysses and Conci, 2010; Richardson and Iain, 2003**, works by taking the absolute value of

the difference between each pixel in the template of original image (I_1) and the corresponding pixel in the matching window of transformed image for comparison (I_2) as shown in **Fig 12**.These differences are summed to get the similarity value of center point in matching window, with each move of the matching window inside the search window, the sum absolute difference between template and match window has been determined. The position where the sum absolute difference reaches its lowest value represents more similar point and its position achieves the best match /fit.

$$SAD = \sum_{(i,j \in \cup)} | I_1(x+i, y+j) - I_2(x+dx+i, y+dy+j) | \quad (22)$$

A new representation of the shift map operation is described by using second order polynomial to improve matching strategy. After determining the more similar point to CPs, we calculate the shift value for them in both X-axis and Y-axis, then calculate the parameter of polynomial transformation function use **Eq. (23) and (24)**, thereafter determine the shift value of each pixel in transformed image by 2nd order polynomial transformation function. Finally, the shift map (is the relative shift of every pixel in the output image from its source in an input image) was used to apply the geometric rearrangement of the transformed image. The relationship between an input image I (x, y) and an output image B(u, v) in image rearrangement and retargeting is defined by a shift-map M(u, v) = (t_x, t_y) as shown in **Fig.13**. The output pixel B (u, v) will be derived from the input pixel I (x + t_x , y + t_y).and the 2nd order polynomial can be expressed as shown below:

$$\Delta X = a_{00} + a_{10}x + a_{11}y + a_{20}x^2 + a_{21}xy + a_{22}y^2 \quad (23)$$

$$\Delta Y = b_{00} + b_{10}x + b_{11}y + b_{20}x^2 + b_{21}xy + b_{22}y^2 \quad (24)$$

where

xy : are the coordinates in the transformed image system

$\Delta X\ \Delta Y$: are the shifts magnitudes

a_{00} ... b_{00}.. : are the transformation coefficients

3. RESULTS

To evaluate the accuracy of the proposed registration approach, the Root Mean Square Error RMSE was calculated to determine the quality of the developed registration process **Congalton, 2009**:

$$RMSE = \sqrt{\frac{1}{N}\sum_{i=1}^{n}((X_i - X_i')^2 + (Y_i - Y_i')^2)} \quad (25)$$

where N is the total number of matched control points, the (X_i , Y_i) are coordinates of control points in the reference image, and the (X_i',Y_i') are the estimated coordinates of the corresponding point in the sensed image based on the transformation model.

The RMSE results of the developed approach (second stage), compared with the traditional registration (first stage), are shown in **Table 7**. It can be observed that image registration using the adjusted registration process results has a lower RMSE values than traditional registration by around 60%, 57% and 48% sequentially for each one of the three tested datasets. Furthermore, the visual results of the three data sets of multi-source (Ikonos, Spot, Quick bird satellite image and LiDAR images) are shown in **Fig 14, 15, 16 and 17**. Based on the visual inspection, it can be seen that results of adjusted registration are more accurate and valid for all datasets.

4. CONCLUSIONS

- The adjusted registration method refined the traditional registration and gives less RMSE of matching from many pixels in the traditional registration to fewer pixels in the adjusted registration, percentage 60%, 57% and 48% sequentially for each one of the three dataset use in this paper.
- The developed registration method is more accuracy and efficiency than selection of the CPs manually, because this method reduces the Local error (displacement of the CPs coordinates) therefore we found more refinement when comparing with feature selection manually.
- From the applied statistical tests on the common transformation methods (affine, polynomial, projective and conformal), the results showed that the 2nd order polynomial function is more accurate and more appropriate to use in matching and registration process to correct geometric distortion.
- The registration for LiDAR images is more accuracy than the registration for satellite images and this was clear in the first stages of registration process, and this is due to the high accuracy for LiDAR system and the LiDAR images are comes from the same sensor while the satellite images comes from different sensor (this images was used in dataset in this research).

REFERENCES

Alruzouq, R.I., 2004, *Semi-Automatic Registration of Multi-Source Satellite Imagery with Varying Geometric Resolutions*. Department of Geomatics Engineering, University of Calgary, Canada.

Bartoli, G., 2007, *Image Registration Techniques*, Universit_a degli Studi di Siena, Visual Information Processing and Protection Group.

Brown, L., 1992, *A survey of image registration techniques*, ACM Computing Surveys 24(4): 325-376.

Charles D. Ghilani and Paulr R.Wolf, 2006, *Adjustment Computation Spatial Data Analysis*, fourth edition, published by John Wiley and Soons, Inc., Hoboken, New Jersey and Canada.

Congalton R.G and K. Green, 2009, *Assessing The Accuracy of Remotely Sensed Data*, principles and practices.

Deakin, R.E. 2004, *The standard and Abridged Molodensky Coordinate Transformation Formulae,* Department of Mathematical and Geospatial Sciences, RMIT University pp.121.

Fatiha, M., Miloud, El.M. and Nasreddine, T., 2010, *A rigid image registration based on the Nonsubsampled Contourlet transform and genetic algorithms*, Sensors 2010, 10, 8553-8571, doi: 10.3390/s100908553.

Gang, H. and Yun, Z., 2008, *Wavelet-based image registration technique for high resolution remote sensing images*, Computers & Geosciences 34.1708–1720.

Ghosh, S. K., 1979, *Analytical Photogrammetry*, Pergamon Press, New York, 203 pp.

Habib, A., Lee, Y. and Morgan, M., 2001, *Surface matching and change detection using modified iterative Hough transform for robust parameter estimation*, Photogrammetric Record, 17 (98): 303-315.

Hu, J., et al. 2003, *Approaches to large-scale urban modeling*, Computer Graphics and Applications, IEEE, 23(6), 62-69.

Jensen, R. J (1986), *Introductory Digital Image Processing*, pp (234-258), Prentice-Hall, New Jersey.

Jia, X. (2003) *On error correction and accuracy assessment of satellite imagery registration* journal of the Australian map circle inc

Kumar V., 2012, Forest Inventory Parameters and Carbon Mapping From Airborne LiDAR, Geo-Information Science and Earth Observation of the University of Twente.

Liu, X. 2008, *Airborne LiDAR for DEM Generation: Some Critical Issues*, [Electronic version]. Progress in Physical Geography, 32(1), 31-49.

Luhmann, T.,Robson,S., Kyle,S. and Harley, I., 2011, *Close Range Photogrammetry, Principles, techniques and applications*. Whittles Publishing, Dunbeath, Caithness KW66EG, Scotland, UK. www.whittlespublishing.com.

Martinez, A., Abad, F.J. (2000), *Remote Sensing Image Rectification in an Automatic Way*, Remote Sensing in the 21st.century.

McCullagh, M., 1988, *Terrain and surface modelling systems: theory and practice*, The photogrammetric record, 12(72), 747-779.

Richardson, E. G., Iain, 2003, *H.264 and MPEG-4 Video Compression: Video Coding for Next-generation Multimedia*. Chichester: John Wiley & Sons Ltd.

Sang, L., 2010, *A coarse-to-fine approach for remote-sensing image registration based on a Local method*, International Journal on Smart Sensing and Intelligent Systems Vol. 3, No. 4.

Santhosh Baboo1, S., Renuka Devi2, M., Keith T. Weber, 2010, *An Analysis of Different Resampling Methods in Coimbatore, District*. Global Journal of Computer and Technology vol. 10 Issue15 (ver.1.0).

Schenk, T., 1999, *Digital photogrammetry*, TerraScience.

Singhai, R. and Singhai, J., 2012, *Registration of Satellite Imagery Using Genetic Algorithm* ,Proceedings of the World Congress on Engineering 2012 Vol II WCE 2012, July 4 - 6, 2012, London, U.K.

Ulysses, J. N. and Conci, A., 2010, *Measuring Similarity in Medical Registration*, IWSSIP 2010-17th International Conference on Systems, Signals and Image Processing.

Wade, T., and Sommer, S., 2006. *A to Z GIS. Redlands*: ESRI Press.

Wong, A., 2008, *Efficient FFT-Accelerated Approach to Invariant Optical-LIDAR Registration*. IEEE Transactions on Geoscience and Remote Sensing.

Wong, A., 2007, *ARRSI: Automatic Registration of Remote-Sensing Images*, IEEE Transactions on Geoscience and Remote Sensing, vol.45, no.5.

Zitova, B. and Flusser, J., 2003, *Image registration methods: a survey*, Image and Vision Computing 977–1000.

Table 1. The parameters of common transformation methods**.**

Parameter of transformation	Transformation function			
	Polynomial	Affine	Projective	Conformal
a1	290.4499	285.7838	0.5335	0.5469
a2	0.5328	0.5413	-0.0033	-0.0003
a3	-0.0103	-0.0014	287.6293	
a4	0.0000		-0.0037	
a5	0.0000			
a6	0.0000			
b1	40.1580	38.2148	0.5441	280.7047
b2	-0.0059	-0.0015	40.1622	38.7970
b3	0.5474	0.5492	-0.0000	
b4	0.0000		-0.0000	
b5	0.0000			
b6	-0.0000			

Table 2. Statistical test (P-value) for transformation Functions.

Statistic test of Transformation Function (P-value)					
data set	function	Normality test		Test for two Variances F-test	Test for two samples (T)
		P-value for CPs of the input image after registration	P-value for CPs of the reference image		
From Satellite images	Affine	0.080	0.080	0.996	0.998
	Projective	0.081		0.998	0.997
	Similarity	0.069		0.971	0.995
	Polynomial	0.077		0.998	0.999

Table 3 List of determined parameters of the affine transformation function for the first test set after rejection of the outlier CPs

	After 1st try
a0	712.710143485467
a1	0.938865715880
a2	0.054032096416
b0	139.791791952421
b1	-0.055409236370
b2	0.938147043380

Table 4. List of determined parameters of the affine transformation function for the second test data.

	1st try	2nd try	3rd try
a0	274.754234133331	277.989788041552	279.8225439838
a1	0.553534903583065	0.550614983484924	0.54683422990834
a2	3.79930994934679E-03	5.37154906337874E-04	7.89680002129255E-04
b0	36.5435927227175	35.8653071871626	36.2180616016215
b1	1.12075860510604E-04	7.24193483558933E-04	-3.49615769592351E-06
b2	0.549094685011655	0.549094685011655	0.549827151117229

Table 5. List of determined parameters of the affine transformation function for the third test data LiDAR.

	1st try
a0	19.2314384309789
a1	0.998351120839234
a2	2.31913326432581E-02
b0	360.118951765439
b1	-6.74618282949926E-03
b2	1.0064727707664

Table 6. List of determined parameters of the 2nd order polynomial transformation for second stage of adjusted registration.

	first test	second test	third test
a0	2.18282	-0.95978	87.33501
a1	-0.00148	0.00379	-0.28481
a2	-0.00651	-0.00085	-0.01376
a3	0.00000	-0.00001	0.00001
a4	0.00000	0.00000	0.00025
a5	0.00000	0.00000	0.00000
b0	-3.50464	-0.31758	-151.91735
b1	0.0072	-0.001	0.58212
b2	0.0021	-0.00044	0.00378
b3	0.00000	-0.00001	0.00001
b4	0.00000	0.00000	-0.00057
b5	0.00000	0.00001	0.00000

Table 7. RMSE values of the manual/classical and the developed methods.

Classical Registration				The proposed approach
Data set	Source data	No. of points of manual selection	RMSE(pixel) For first stage	RMSE(pixel) For second stage
First test	Satellite images	43	2.323	0.932
Second test	Satellite images	35	3.653	1.564
Third test	LiDAR images	14	1.871	0.987

(a) **(b)**

Figure 1. Spot and Quick Bird satellite images.

(a) **(b)**

Figure 2. Ikonos and Quick Bird satellite images.

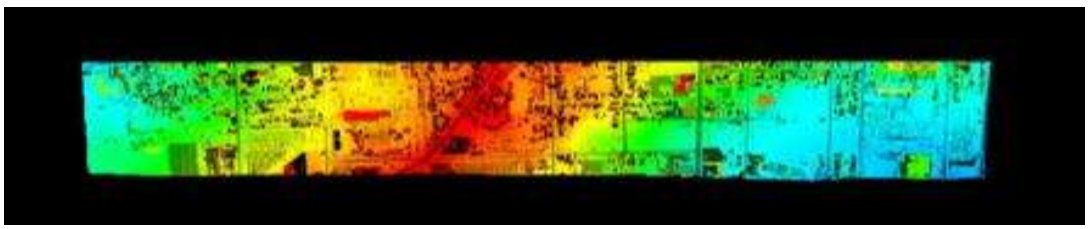

a.Strip_1

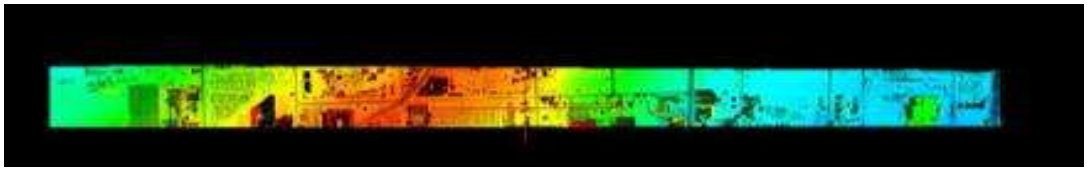

b.Strip_2

Figure 3. Laser point clouds dataset, a.Strip_1, and b.Strip_2.

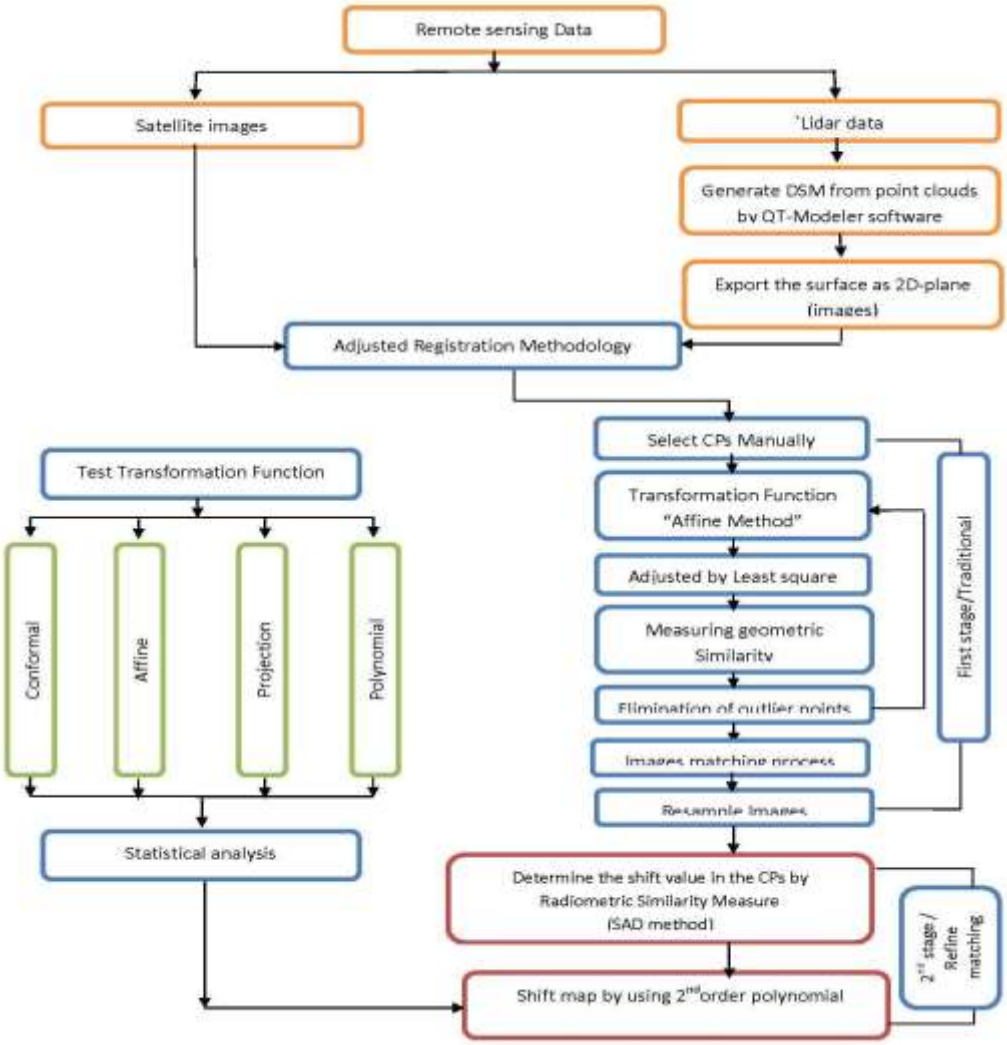

Figure 4. The workflow of the adjusted registration.

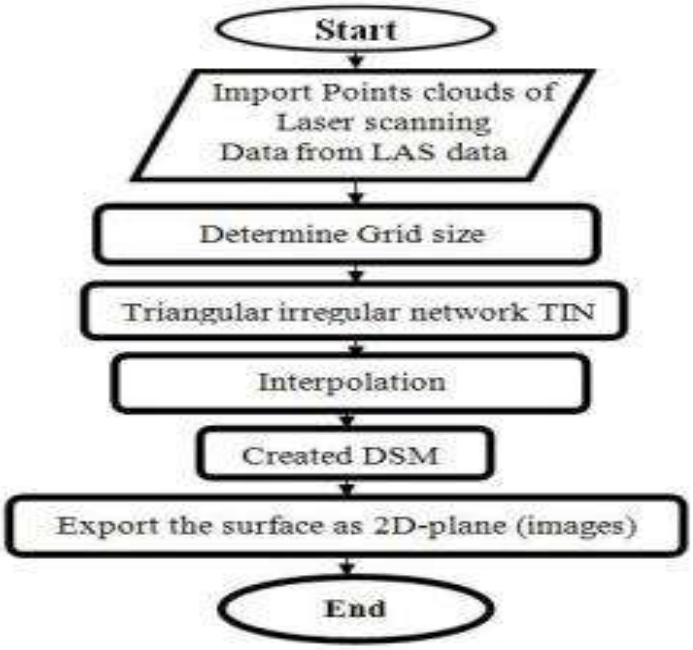

Figure 5. Transform 3D LiDAR data to 2D image.

a. Reference image **b. sensed image**

Figure 6. Manual extraction of control points in reference and sensed image.

(a) (b)

Figure 7. Manual extraction of control points in reference and sensed image.

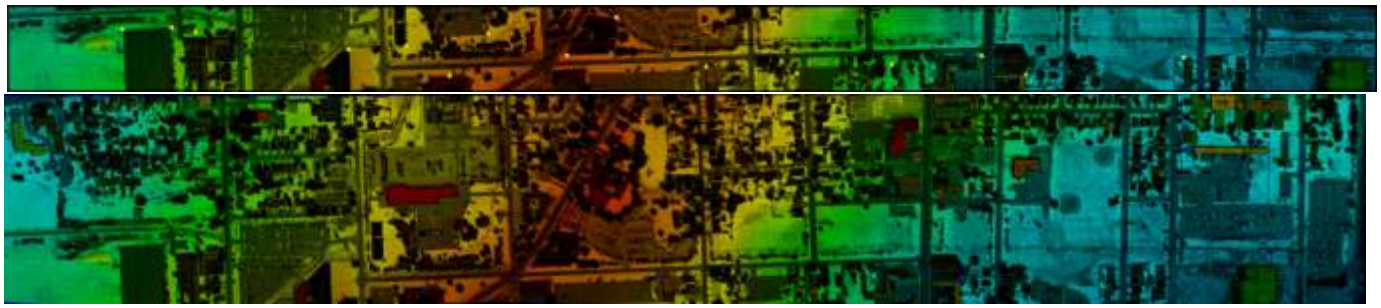

Figure 8. Manual extraction of control points in reference and sensed image.

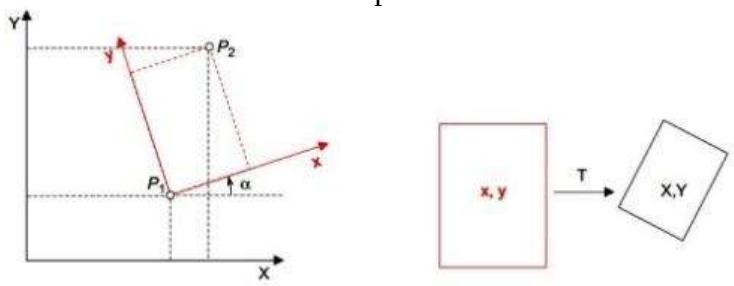

Figure 9. Plane similarity transformations (Luhmann et al., 2011).

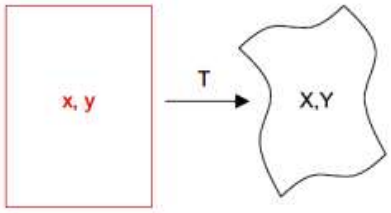

Figure 10. Plane polynomial transformations (Luhmann et al., 2011).

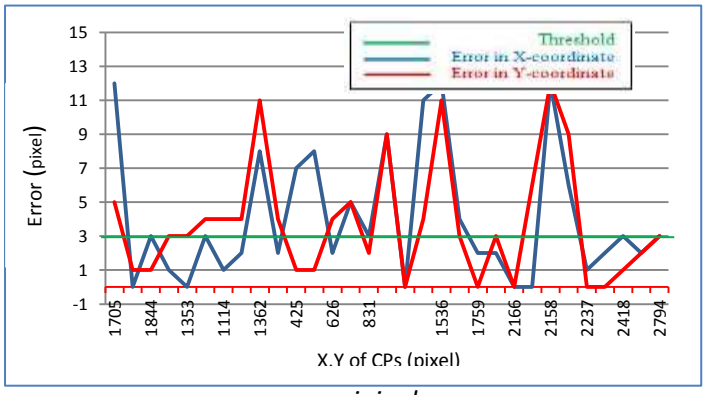

a.original

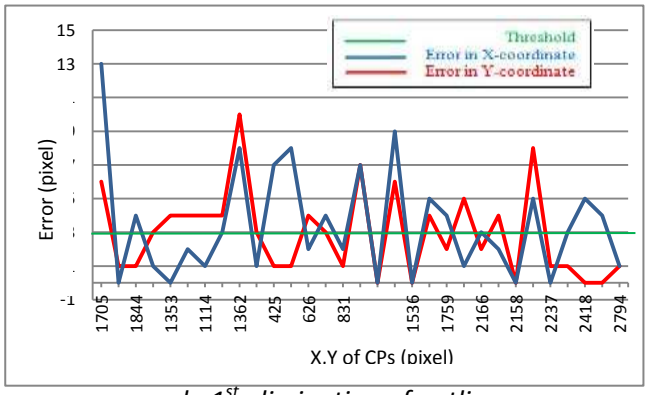

b. 1st elimination of outlier

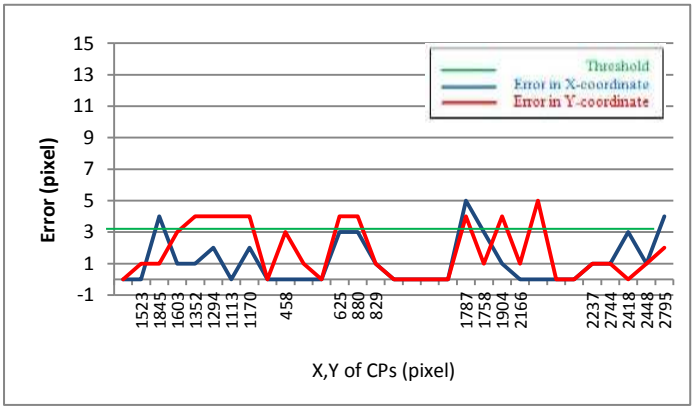

c. 2nd elimination of outlier

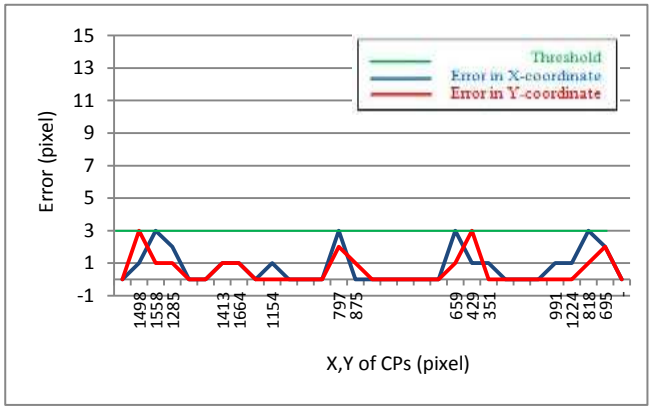

d. 3rd elimination of outlier

Figure 11. The elimination process of outlier points over threshold

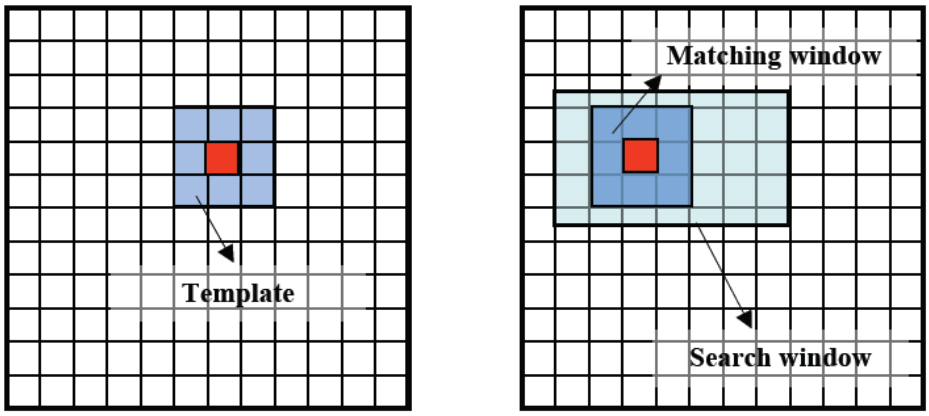

Reference Image (I_1) **Input Image (I_2)**

Figure 12. Concept of radiometric similarity measure (Alruzouq, 2004)**.**

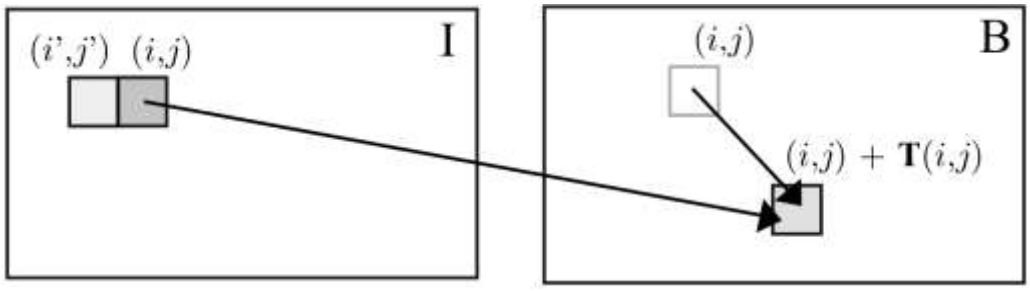

Figure 13. Shift-map between two images.

a. first stage /traditional registration b. second stage /adjusted registration

Figure 14. Image matching results between the image from spot satellite as reference image and quick bird satellite as sensed image a. the first stage /traditional registration b. second stage of image registration adjustment.

a. first stage /traditional registration b. second stage /adjusted registration

Figure 15. Image matching results between the image from spot satellite as reference image and quick bird satellite as sensed image a. the first stage /traditional registration b. second stage of image registration adjustment.

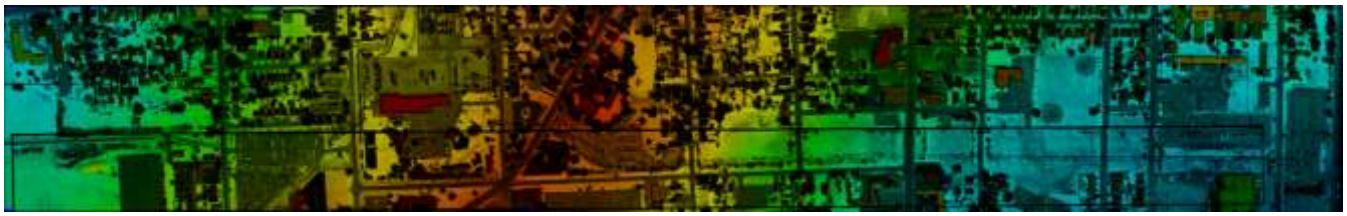

Figure 16. The image matching results between the strip 1 as reference image and strip 2 as sensed image (the first stage /traditional image registration).

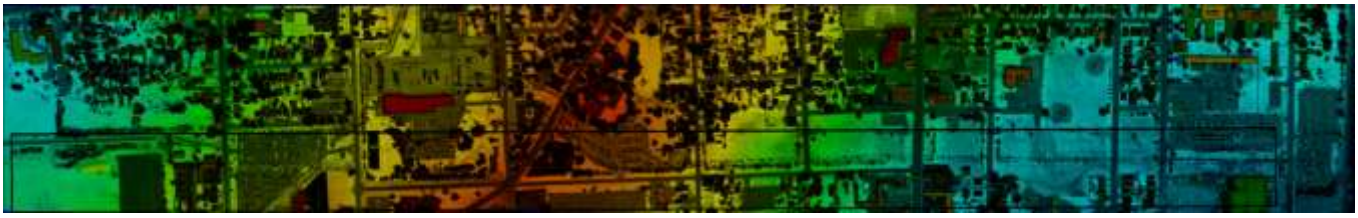

Figure 17. The image matching results between the strip 1 and strip 2 images

(second stage / adjusted registration process).